Transactions of the Korean Nuclear Society Autumn Meeting
Gyeongju, Korea, October 29-30, 2015

Evaluation of Fuel Performance Uncertainty in a PWR HFP RIA Analysis

Joosuk Lee and Swengwoong Woo
Korea Institute of Nuclear Safety
62 Gwahak-ro, Yusong-gu, Daejeon, 305-338, Republic of Korea
Tel: +82-42-868-0784, Fax: +82-42-868-0045
Email: jslee2@kins.re.kr

1. Introduction

Approved analysis methodology for licensing application in the safety analysis of reactivity initiated accident (RIA) in Korea is based on a conservative approach. But newly introduced safety criteria, described in section 4.2 of NUREG-0800, tend to reduce the margins or depending on the reactor types rod failure is predicted due to the pellet-to-cladding mechanical interaction (PCMI) criteria [1]. Thereby, licensee is trying to improve the margins by utilizing a less conservative approach. For example, a 3D kinetic analysis approach has been developed in U.S. and it is also developing in Korea for licensing application [2,3]. In this situation, to cope with this technological transition, KINS has been also developing a new audit calculation methodology based on a realistic approach [4].

Realistic approach is a well-known methodology for the area of loss-of-coolant accident (LOCA) safety analysis, and it believes that approach can possibly be applicable to the RIA safety analysis area also. Realistic approach is composed of the evaluation of best-estimate performance and uncertainty quantification. Best-estimate performance can be obtained by use of the best-estimate computer codes. Best-estimate computer codes have to describe fuel behaviors during RIA with a sufficient accuracy. For the assurance of accuracy, computer codes have to be validated with the sufficient amount of experiment data. And for the uncertainty quantification, uncertainty parameters and ranges of uncertainty must be identified, and combined uncertainty has to be evaluated with a appropriate statistical treatment.

Author previous work identified as many as uncertainty parameters which may affect the fuel performance during RIA. And their effects on rod performance during a hot zero power (HZP) RIA have been analyzed [5]. Analysis results revealed that power related uncertainties such as the peak power and full width half maximum (FWHM) showed relatively strong influences to the rod performance. And several uncertainty parameters in manufacturing and also in models have showed strong impacts. But, as usual, the impacts of these parameters can be affected depending on the initial states of fuel rod and rated fuel power before RIA.

Thereby, in this paper, further sensitivity studies based on the various kinds of uncertainty have been carried out again in a PWR hot full power (HFP) condition. And effects of combined uncertainty have been evaluated by utilizing a non-parametric order statistics approach as well.

2. Analysis Details

2.1 Base case analysis

In this study, Westinghouse-type 17x17 fuel with Zircaloy-4 cladding was utilized. Design parameters of fuel rod, operating conditions, and base irradiation power history were the same as the authors' previous works and these are obtained from NUREG-1754 [6]. Initiation of RIA was supposed to occur at the fuel burnup of 0.5 and 30 MWd/kgU, respectively. Applied power pulse during HFP RIA was obtained from the beginning of life full power RIA analysis in AP1000 reactor [7]. Slightly top-skewed cosine-like axial power profile was used before the initiation of RIA and a single strongly top-skewed imaginary axial power profile was utilized in the period of RIA. Applied rod averaged power pulses and axial power profile were shown in Fig.1. Local peak linear heat rate before RIA was set as 14.0 kW/ft. In this way, radially averaged total injected energy at the axially hottest spot of the fuel rod up to the time of 10 sec after accident initiation was 101.8 cal/g.

For the fuel performance assessment, FRAPCON-3.4a and FRAPTRAN-1.5 code were used.

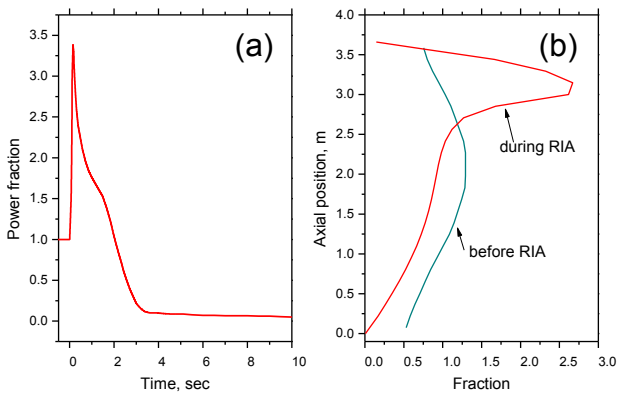

Fig. 1 (a) Applied rod averaged power fraction during RIA, and (b) axial power profiles for RIA analysis. Accident initiated at the time of t=0s.

20 evenly spaced axial nodes in the fuel rod and 20 equal-area radial nodes in a pellet were used. 'Coolant option' in FRAPTRAN code input was turned on to specify the coolant conditions for RIA analysis.

2.2 Sensitivity and combined uncertainty analysis

Considered uncertainty parameters for the sensitivity study were 45 parameters and these can be categorized as manufacturing, models in computer code, thermal-hydraulic boundary conditions and fuel power. All these parameters are already identified in previous work [6]. Detailed information on the parameter including their uncertainties is listed in Table 1.

Effects of combined uncertainty were evaluated by utilizing a non-parametric order statistics approach. Non-parametric order statistics based on the Wilks' formula is a well-known statistical method for the best-estimate LOCA safety analysis, and its validity is already proven through the OECD/NEA BEMUSE program [8]. Several sets of 124 inputs for the running of FRAPCON/FRAPTRAN were produced by utilizing a simple random sampling (SRS) technique [9].

3. Results

3.1 Base case

Fig. 2 shows the evolution curves of radial averaged peak fuel enthalpy, peak cladding hoop strain increment, peak fuel and cladding temperature with changing fuel burnup. These peak values were obtained at the axial node number of 13 from the bottom position of fuel rod. As can be seen in Fig. 2(a), the peak enthalpy was 101.3 and 108.0 cal/g at the fuel burnup of 0.5 and 30 MWd/kgU, respectively. This result indicates that at the given analysis condition, the peak enthalpy of 30 MWd/kgU fuel burnup showed a little bit higher value than the result of 0.5 MWd/kgU condition. This seems to be related to the thermal conductivity degradation of UO_2 fuel with fuel burnup increase.

Fig. 2(b) shows the evolution curves of peak fuel temperature. As coincided with the the results of enthalpy, peak fuel temperature of 30 MWd/kgU burnup was somewhat higher than the results of 0.5 MWd/kgU condition. It was 2431.4 and 2498.0 K at the fuel burnup of 0.5 and 30 MWd/kgU, respectively.

Fig. 2(c) shows the evolution of clad hoop strain increment. Peak clad hoop strain increment was 0.13 and 0.38% at the fuel burnup of 0.5 and 30 MWd/kgU, respectively. This difference is mostly originated from the difference of initial gap size before RIA.

Fig. 2(d) shows the evolution of peak cladding temperature. At the fuel burnup of 0.5 MWd/kgU, peak cladding temperature was 824.7 K and as fuel burnup moved to 30 MWd/kgU, it was 818.4 K. In the FRAPTRAN code, the temperature rise effect due to the oxide layer formation was not factorized properly in the transient mode. Therefore as the transient mode was activated at the time of 0 sec, about 20K drop of

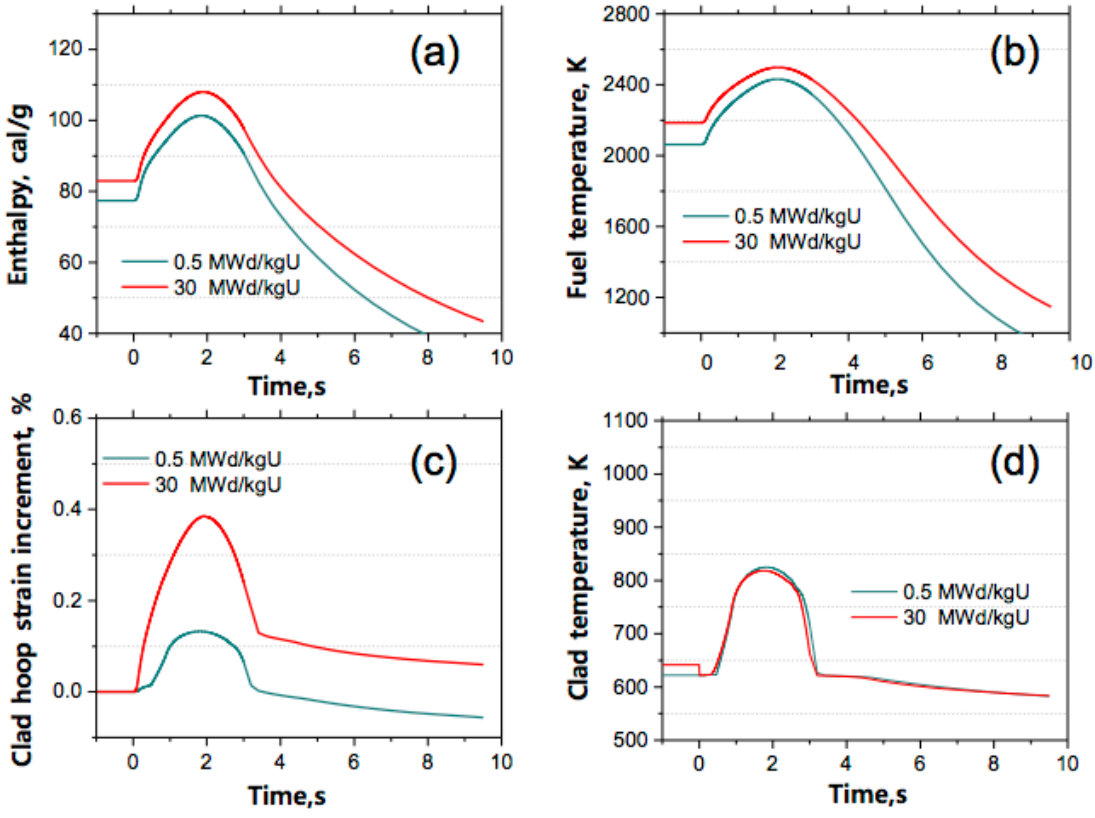

Fig. 2. Evolution curves of (a) radial averaged peak fuel enthalpy, (b) peak fuel temperature, (c) peak cladding hoop strain increment and (d) peak cladding temperature with changing fuel burnup. RIA was initiated at the time of t=0 s.

Table 1. Effects of fuel rod uncertainty on the peak fuel enthalpy (Δh), peak cladding hoop strain increment (Δε_hp), peak fuel (ΔPFT) and peak cladding temperature (ΔPCT) as a function of fuel burnup.

	Parameter	Tolerance or Bias	0.5 MWd/kgU				30 MWd/kgU			
			Δh, cal/g	Δε_hp, %	ΔPFT, K	ΔPCT, K	Δh, cal/g	Δε_hp, %	ΔPFT, K	ΔPCT, K
Manufacturing	1. Cladding inner diameter, mm	±0.04	12.7	0.10	171.1	7.8	0.3	0.00	1.7	4.8
	2. Cladding thickness, mm	±0.04	0.6	0.00	10.1	2.2	0.4	0.01	7.3	3.2
	3. Cladding roughness, micron	±0.3	0.0	0.00	0.0	0.0	0.0	0.00	0.2	0.1
	4. Pellet outer diameter, mm	±0.013	4.7	0.00	59.1	1.6	0.2	0.00	0.8	2.6
	5. Pellet density, %	±0.91	1.4	0.00	36.0	0.7	2.7	0.01	46.5	0.6
	6. Pellet re-sinter density increase, %	±0.4	3.6	0.00	39.4	0.1	1.1	0.00	19.4	1.1
	7. Pellet roughness, micron	±0.5	0.0	0.00	0.1	0.0	1.2	0.00	14.2	0.3
	8. Pellet dish diameter & depth, mm	±0.5, +0.05	0.0	0.00	0.2	0.0	0.0	0.00	0.2	0.0
	9. Rod fill pressure, Mpa	±0.07	0.3	0.00	2.4	0.8	0.1	0.00	1.1	0.0
	10. Rod plenum length, mm	±11.4	0.1	0.00	1.2	0.2	0.1	0.00	0.8	0.0
Model	11. Fuel thermal conductivity	±2σ	11.9	0.06	319.1	11.9	25.4	0.01	461.6	8.8
	12. Fuel thermal expansion	±2σ	10.3	0.14	135.2	3.2	0.2	0.16	0.1	2.6
	13. FGR	±2σ	0.0	0.00	0.0	0.0	2.4	0.00	27.2	0.9
	14. Fuel swelling	±2σ	0.0	0.00	0.0	0.0	0.1	0.00	0.2	0.9
	15. Fuel relocation	±2σ(±34%)	0.0	0.00	0.4	0.0	0.0	0.00	0.0	0.3
	16. Fuel specific heat capacity	±1se	1.6	0.00	5.2	1.2	1.7	0.01	4.4	1.0
	17. Fuel emissivity	±1se	0.0	0.00	0.0	0.0	0.0	0.00	0.0	0.0
	18. Cladding corrosion(oxide thickness)	±2σ	0.3	0.01	11.0	5.1	3.4	0.01	47.8	7.2
	19. Creep of cladding	±2σ	1.2	0.00	12.8	0.7	0.0	0.00	0.1	0.5
	20. Cladding axial growth	±2σ	0.1	0.00	1.0	0.2	0.0	0.00	0.1	0.0
	21. Hydrogen pickup	±2σ	0.0	0.00	0.0	0.0	0.0	0.00	0.0	0.0
	22. Cladding thermal conductivity	±2σ	0.8	0.00	11.4	0.9	1.3	0.00	15.5	1.3
	23_1 Cladding axial thermal expansion	±30%	0.0	0.00	0.4	0.1	0.0	0.00	0.2	0.0
	23_2 Cladding diametral thermal expansion	±30%	3.0	0.08	34.0	3.5	0.0	0.01	0.1	0.3
	24. Cladding elastic modulus	±1se	0.8	0.01	8.7	0.8	0.0	0.02	0.2	0.0
	25. Cladding specific heat	±1se	0.0	0.00	0.0	0.7	0.0	0.00	0.0	0.8
	26. Cladding yield stress	±30%	0.0	0.00	0.0	0.0	0.0	0.01	0.0	0.2
	27. Cladding surface emissivity	±1se	0.0	0.00	0.2	0.0	0.0	0.00	0.0	0.0
	28. Zirconium oxide thermal conductivity	0.5~1.1	0.2	0.00	0.6	1.1	1.7	0.01	23.5	4.7
	29. Gas conductivity (He)	±2σ	0.3	0.00	4.1	0.6	0.1	0.00	0.8	0.4
	30. Cladding failure stress, MPa	-30 ~ +90	0.0	0.00	0.0	0.0	0.0	0.00	0.0	0.0
	31. Cladding failure strain	0.2~1.6	0.0	0.00	0.0	0.0	0.0	0.00	0.0	0.0
	32. High temperature oxidation (C-P)	±6%	0.0	0.00	0.0	0.0	0.0	0.00	0.0	0.0
	33. Crud thermal conductivity	0.5~1.5	0.0	0.00	0.0	0.0	0.0	0.00	0.0	0.0
	34. Crud thickness(accumarated), micron	0~30	0.2	0.00	0.9	1.2	4.4	0.01	55.1	12.9
	35. Dittus-Boelter HTC(liquid)	0.6~1.4	0.2	0.00	0.2	1.1	0.2	0.00	0.1	1.6
	36. Dittus-Boelter HTC(vapor)	0.6~1.4	0.0	0.00	0.0	0.0	0.0	0.00	0.0	0.0
	37. EPRI-1 CHF	0.2~1.8	8.8	0.12	10.4	210.9	7.0	0.07	5.3	201.9
	38. Tom HTC	0.5~1.5	1.1	0.02	0.3	38.5	1.1	0.01	0.2	40.5
	39. Groenveld HTC	0.5~1.5	6.5	0.09	0.0	237.7	6.1	0.01	0.0	232.5
TH BC	40. Coolant temp.,K	±3	0.9	0.00	1.5	5.3	1.0	0.01	0.9	8.1
	41. Coolant pressure, MPa	±0.15	0.6	0.01	0.0	10.9	0.5	0.01	1.2	12.4
	42. Mass flow rate	0.98~1.02	0.7	0.01	0.8	9.3	0.7	0.01	0.4	11.0
Power	43. radial power profile	0.9~1.1	1.0	0.00	66.1	1.8	2.2	0.01	60.2	4.3
	44. Power(peak power)	0.95~1.05	11.0	0.04	146.0	47.9	12.8	0.18	125.4	41.6
	45. FWHM	0.95~1.05	4.2	0.01	70.2	17.8	4.7	0.08	61.4	15.5
Base case			h, cal/g	ε_hp, %	PFT, K	PCT, K	h, cal/g	ε_hp, %	PFT, K	PCT, K
			101.3	0.13	2431.4	824.7	108.0	0.38	2498.0	818.4

cladding temperature was observed at the fuel burnup of 30 MWd/kgU, shown in Fig 2(d).

3.2 Sensitivity anaysis

3.2.1 Peak fuel enthalpy

Analysis results of fuel rod uncertainty to the changes of peak fuel enthalpy (Δh) were summarized in Table 1. At the fuel burnup of 0.5 MWd/kgU, pellet outer diameter, pellet re-sinter density increase, cladding thermal expansion, EPRI-1 CHF correlation, Groenveld 5.9 HTC correlation and FWHM showed a moderate influence to the Δh. They induced about 3.0~8.8 cal/g Δh. Meanwhile uncertainties of cladding inner diameter, fuel thermal conductivity, fuel thermal expansion and peak power have induced a significant impact. They resulted in 10.3~12.7 cal/g Δh.

As fuel burnup moved to 30 MWd/kgU, cladding corrosion, crud thickness, EPRI-1 CHF, Groenveld 5.9 HTC correlation, FWHM have induced a moderate influence. They resulted in 3.4~7.0 cal/g Δh. But fuel thermal conductivity and peak power still showed a strong influence. Particularly fuel thermal conductivity revealed a very strong impact. It showed 25.4 cal/g Δh.

3.2.2 Peak hoop strain increment

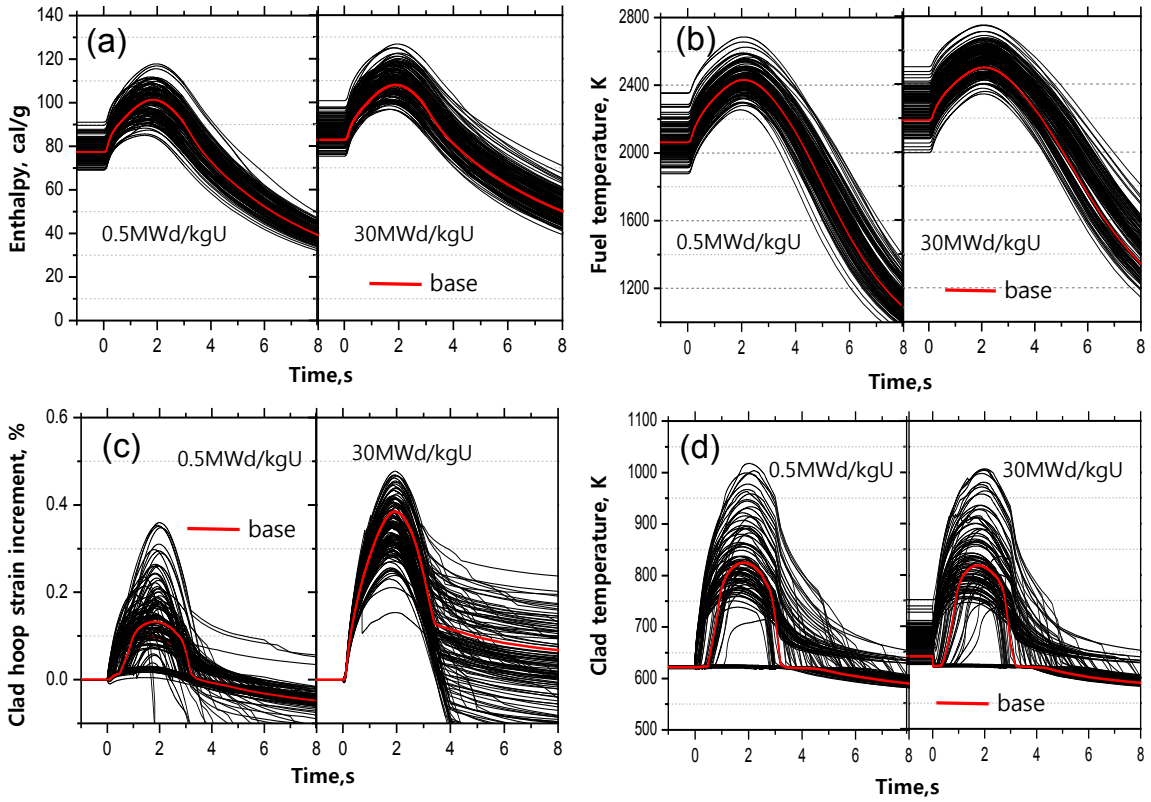

Fig. 3. A set of 124 fuel performance evolution curves. (a) peak enthalpy, (b) peak fuel, (c) peak cladding hoop strain increment and (d) peak cladding temperature with burnup change.

At the fuel burnup of 0.5 MWd/kgU, cladding inner diameter, fuel thermal expansion, EPRI-1 CHF showed a relatively strong influence to the change of cladding hoop strain increment(Δε_hp). They showed about 0.1~ 0.14 % Δε_hp. But the others were less significant, less than 0.1%. And as burnup moved to 30 MWd/kgU, fuel thermal expansion and peak power induced a strong influence such that it was 0.16~0.18% Δε_hp. And effects of the others were also not significant.

3.2.3 Peak fuel temperature

Change of peak fuel temperature (ΔPFT) was also summarized in Table 1. At the 0.5 MWd/kgU burnup, pellet outer diameter, radial power profile, FWHM showed a moderate influence to the ΔPFT. It was about 60~70K. Cladding inner diameter, fuel thermal conductivity, fuel thermal expansion, peak power have induced a strong influence. ΔPFT was about 135~320K.

As fuel burnup moved to 30 MWd/kgU, pellet density, cladding corrosion, crud thickness, radial power profile and FWHM resulted in a moderate influence. ΔPFT was about 50~60 K. But again fuel thermal conductivity and peak power showed a strong impact. Especially fuel thermal conductivity has induced very strong impact. It was about 460 K ΔPFT.

3.2.4 Peak cladding temperature

At the fuel burnup of 0.5 and 30 MWd/kgU, Tom HTC correlation and peak power showed a moderate influence to the change of peak cladding temperature (ΔPCT). ΔPCT was about 40~50 K, irrespective of fuel burnup. However, EPRI-1 CHF and Groenveld-5.9 correlation have induced very strong impact, irrespective of fuel burnup also. ΔPCT was about 210~240 K.

3.3 Combined uncertainty

Fig. 3(a) shows a set of 124 fuel enthalpy evolution curves. At the 0.5 MWd/kgU condition, the minimum and maximum peak enthalpy was 117.8 and 85.0 cal/g, respectively. And at the 30 MWd/kgU, it was 126.8 and 96.7 cal/g. Thus the change of peak enthalpy was about 30 cal/g, irrespective of fuel burnup.

Fig. 3(b) shows the peak fuel temperature evolution curves. At the 0.5 MWd/kgU condition, the minimum and maximum peak fuel temperature was 2254.5 and 2685.4 K, respectively, and at the 30 MWd/kgU condition it was 2342.2 and 2748.5 K. Thus it varied about 400K.

Fig. 3(c) shows cladding hoop strain increment curves. At the fuel burnup of 0.5 MWd/kgU, the minimum and maximum hoop strain increment was 0.0 and 0.36%. And, as burnup moved to 30 MWd/kgU, it was ranging from 0.22 to 0.48 %. Thus permanent hoop strain varied about 0.3~0.4%.

Fig. 3(d) shows the peak cladding temperature evolution curves. At the 0.5 MWd/kgU condition, the minimum and maximum peak cladding temperature was

621.9 and 1017.5 K, respectively. And it was 621.9 and 1006.6 K for the 30 MWd/kgU condition. Thus the change of peak cladding temperature was about 400K. However the minimum cladding temperature seems to be too low, and this is mostly caused by the uncertainty parameter of EPRI-1 CHF correlation. Therefore uncertainty range on this parameter has to be validated for further analysis. And as stated in section 3.1, the maximum cladding temperature of 30 MWd/kgU burnup must be increased further because the temperature rise effects due to the formation of oxide and crud layer was not factorized properly in the code.

Analysis results of combined uncertainty reveal that fuel performance during HFP RIA can be affected significantly by the various sources of uncertainty. Therefore to obtain more accurate analysis results, determination of exact range of uncertainty on the key uncertainty parameters has to be done.

4. Summary

Sensitivity and combined uncertainty studies based on the various kinds of uncertainty sources have been carried out in a PWR hot full power (HFP) condition. Main findings are as follows.

- Cladding inner diameter, fuel thermal conductivity, fuel thermal expansion and peak power have induced a significant impact to the fuel enthalpy and temperature.
- Cladding hoop strain was strongly affected by the uncertainty parameters of cladding inner diameter, fuel thermal expansion, EPRI-1 CHF and peak power.
- As expected, heat transfer correlations such as EPRI-1 CHF and Groenveld 5.9 have induced a strong impact to the cladding temperature.
- Fuel performance parameters such as enthalpy, fuel and cladding temperature were greatly affected by the combined uncertainty. Therefore determination of exact ranges of uncertainty will be required for further detailed analysis.
- Above results are valid in the given analysis condition in this paper. Thereby, the analysis conditions, for example the peak linear heat rate before RIA or peak power and FWHM etc, are changed the results will be changed also.

REFERENCES

1. Jaeil Lee, “반응도인가사고 허용요건 및 현안”, Symposium on Nuclear Safety Analysis, June 2009
2. EPRI, “RETRAN-3D Analysis of BWR Control Rod Drop Accidents”, 1015206, June 2007
3. Jaeil Lee, “ 반응도사고 해석을 위한 발전방향”, Symposium on Nuclear Safety Analysis, July 2015.
4. Joosuk Lee et. al., “ Development of Aduit Calculation Methodology for RIA Safety Analysis, Transaction of the Korean Nuclaer Society Spring Meeting, Jeju, Korea, May 7-8, 2015
5. Joosuk Lee, Swengwoong Woo, “Effects of Fuel Rod Uncertainty in PWR HZP RIA Analysis”, Topfuel 2015, Zurich, Switzerland, 13-17 September 2015 (to be presented)
6. O’Donnell, G.M., Scott, H.H., Meyer, R.O., 2001, “A New Comparative Analysis of LWR Fuel Designs”, NRC, NUREG-1754
7. “CONTROL ROD EJECTION”, AP1000 Design Control Document Rev.19, Chapter 15, Westinghouse Electric Company, 2005 (http://pbadupws.nrc.gov/docs/ML1117/ML11171A371.pdf)
8. OECD/NEA, “BEMUSE PHASE III REPORT; Uncertainty and Sensitivity Analysis of the LOFT L2-5 Test”, NEA/CSNI/R(2007)4, 2007
9. Iman, R.L., Shortencarier, M.J., 1984, “FORTRAN 77 Program and User's Guide for the Generation of Latin Hypercube and Random Samples for Use with Computer Models”, NRC, NUREG/CR-3624